



HAL
open science

Estimating the macroscopic capillary length from Beerkan infiltration experiments and its impact on saturated soil hydraulic conductivity predictions

Simone Di Prima, Ryan Stewart, Mirko Castellini, Vincenzo Bagarello, Majdi Abou Najm, Mario Pirastru, Filippo Giadrossich, Massimo Iovino, Rafaël Angulo-Jaramillo, Laurent Lassabatère

► To cite this version:

Simone Di Prima, Ryan Stewart, Mirko Castellini, Vincenzo Bagarello, Majdi Abou Najm, et al.. Estimating the macroscopic capillary length from Beerkan infiltration experiments and its impact on saturated soil hydraulic conductivity predictions. *Journal of Hydrology*, 2020, 589, pp.125159. 10.1016/j.jhydrol.2020.125159 . hal-02883951

HAL Id: hal-02883951

<https://univ-lyon1.hal.science/hal-02883951>

Submitted on 7 Jan 2021

HAL is a multi-disciplinary open access archive for the deposit and dissemination of scientific research documents, whether they are published or not. The documents may come from teaching and research institutions in France or abroad, or from public or private research centers.

L'archive ouverte pluridisciplinaire **HAL**, est destinée au dépôt et à la diffusion de documents scientifiques de niveau recherche, publiés ou non, émanant des établissements d'enseignement et de recherche français ou étrangers, des laboratoires publics ou privés.

1 **Estimating the macroscopic capillary length from Beerkan infiltration experiments**

2 Simone Di Prima ^{a,b*}, Ryan D. Stewart ^c, Mirko Castellini ^d, Vincenzo Bagarello ^e, Majdi R. Abou Najm ^f, Mario
3 Pirastru ^a, Filippo Giadrossich ^a, Massimo Iovino ^e, Rafael Angulo-Jaramillo ^b and Laurent Lassabatere ^b

4 ^a Department of Agricultural Sciences, University of Sassari, Viale Italia, 39, 07100 Sassari, Italy.

5 ^b Université de Lyon; UMR5023 Ecologie des Hydrosystèmes Naturels et Anthropisés, CNRS, ENTPE, Université Lyon 1, Vaulx-
6 en-Velin, France.

7 ^c School of Plant and Environmental Sciences, Virginia Polytechnic Institute and State University, Blacksburg, VA, United State.

8 ^d Council for Agricultural Research and Economics-Agriculture and Environment Research Center (CREA-AA), Via Celso Ulpiani
9 5, 70125 Bari, Italy.

10 ^e Department of Agricultural, Food and Forest Sciences, University of Palermo, Palermo, Italy.

11 ^f Department of Land, Air and Water Resources, University of California, Davis, CA 95616, United States.

12 * Corresponding Author. E-mail: sdiprima@uniss.it

13 **Abstract**

14 In this investigation, we propose a simple field method for estimating the macroscopic capillary
15 length, λ_c , by only using a single-ring infiltration experiment of the Beerkan type and a measurement
16 of the initial and saturated soil water contents. We assumed that the intercept of the final portion of
17 an experimental infiltration curve could be used as a reliable predictor of the macroscopic capillary
18 length. This hypothesis was validated by assessing the proposed calculation approach using both
19 analytical and field data. The analytical validation demonstrated that the proposed method was able
20 to provide reliable λ_c estimates over a wide range of soil textural characteristics and initial soil water
21 contents. The field testing was performed on a large database including 433 Beerkan infiltration
22 experiments, with the 99.1% of the experiments yielding realistic λ_c values. This method constitutes
23 an easy solution for estimating λ_c , and it can be applied in conjunction with a number λ_c -dependent
24 methods for estimating the saturated soil hydraulic conductivity, K_s , allowing to improve K_s
25 prediction in the field.

26 **Keywords:** infiltration, macroscopic capillary length, Beerkan, hydraulic conductivity.

27

28 1. Introduction

29 Gardner (1958) proposed an exponential relation between the soil hydraulic conductivity, K (L T⁻¹) and the water pressure head, h (L):

$$31 \quad K(h) = K_s \exp(\alpha h) \quad (1)$$

32 where K_s (L T⁻¹) is the saturated soil hydraulic conductivity and α (L⁻¹) is a fitting parameter. Many
33 authors pointed out the importance of the α parameter. For instance, Philip (1985) introduced a
34 parameter related to α called sorptive length that expresses the role of sorption in multidimensional
35 (2-3D) steady state flows. The reciprocal of α , i.e., the macroscopic capillary length, λ_c (L), is a more
36 general length scale parameter that was firstly defined as an integral parameter by Bouwer (1964)
37 (called capillary fringe in his work) and later discussed in detail by White and Sully (1987) and Philip
38 (1985). This parameter expresses the relative importance of gravity and capillary forces during water
39 movement in unsaturated soils (Raats, 1976). More specifically, low λ_c values indicate a dominance
40 of gravity over capillarity, which occurs in coarse-textured and/or highly structured porous media.
41 On the contrary, high λ_c values indicate dominance of capillarity over gravity, which occurs in fine-
42 textured and/or unstructured porous media (Reynolds et al., 2002).

43 The λ_c parameter depends on the soil hydraulic characteristics and the initial condition (Smith et
44 al., 2002), and is defined as follows (Philip, 1985):

$$45 \quad \lambda_c = \frac{\phi_m}{\Delta K} \quad (2)$$

46 where $\Delta K (=K_s - K_i)$ stands for the difference between K_s and the initial soil hydraulic conductivity,
47 K_i (L T⁻¹), and ϕ_m (L²T⁻¹) is the matric flux potential, defined by (Gardner, 1958):

$$48 \quad \phi_m = \int_{h_i}^0 K(h) dh \quad h_i \leq h \leq 0 \quad (3)$$

49 where h_i (L) is the initial soil water pressure head.

50 Eq. (1) has been used in numerous studies to solve the flow problem (e.g., Philip, 1968; Wooding,
51 1968). Therefore, the knowledge λ_c has a noticeable practical interest since these parameters were
52 included in many infiltrometer methods for calculating the saturated soil hydraulic conductivity

53 (Bagarello et al., 2004, 2014d, e.g., 2017; Elrick and Reynolds, 1992; Nimmo et al., 2009; Reynolds
54 and Elrick, 1990; Stewart and Abou Najm, 2018a; Wu et al., 1999). Sometimes, its reciprocal, α , is
55 considered, instead.

56 Many infiltrometer techniques have been developed overtime to estimate λ_c (e.g., Bagarello et al.,
57 2013; Reynolds and Elrick, 1990; Stewart and Abou Najm, 2018a; Wu et al., 1999). However, all
58 these methods present some limitation. For instance, the two-ponding depths method by Reynolds
59 and Elrick (1990) requires the execution of complicate experiments in the field for measuring the
60 steady state flow rates corresponding to two ponding depths of water. Bagarello et al. (2013) proposed
61 some empirical equations, that however need to be calibrated on experimental infiltration data.
62 Approach 3 by Stewart and Abou Najm (2018b) uses water retention data to constrain λ_c , thus this
63 method requires the estimation of the $\theta(h)$ relationship. Other methods are based on the analysis of
64 transient state data, as for the case of the method 1 by Wu et al. (1999) and Approach 2 by Stewart
65 and Abou Najm (2018a), that need an accurate and often not easy to obtain description of the transient
66 state (Di Prima et al., 2019). Therefore, alternative methods for estimating λ_c from simple and easily
67 replicable infiltration experiments could substantially reduce the amount of work necessary to obtain
68 accurate estimates of soil hydraulic properties in the field (Bagarello et al., 2014d).

69 The objective of this investigation was to validate a simple field method to estimate the
70 macroscopic capillary length by only using a single-ring infiltration experiment of the Beerkan type
71 (Lassabatere et al., 2006) and a measurement of the initial and saturated soil water contents. The
72 theoretical analysis was initially developed. The proposed method was then validated using
73 analytically generated data and a Beerkan infiltration database including 433 field experiments.

74 2. Theory

75 According to White and Sully (1987), Eq. (2) could be rewritten as:

$$76 \lambda_c = \frac{b S^2}{(\Delta\theta \Delta K)} \quad (4)$$

77 where b is a dimensionless constant dependent on the shape of the soil water diffusivity function, S
 78 ($L T^{-0.5}$) is the soil sorptivity (Philip, 1957), $\Delta\theta$ ($=\theta_s - \theta_i$) stands for the difference between the
 79 saturated, θ_s (L^3L^{-3}), and initial, θ_i (L^3L^{-3}), volumetric soil water content. For field soils, b is
 80 commonly set equal to 0.55 and K_i is negligible (White and Sully, 1992).

81 The estimation of the macroscopic capillary length with equation (4) requires the previous
 82 determination of sorptivity and hydraulic conductivity. These quantities can be estimated thanks to
 83 water infiltration experiments and fitting to the quasi-exact implicit (QEI) model developed by
 84 Haverkamp et al. (1994) or its related approximate expansions (see Lassabatere et al., 2009 for more
 85 details). Haverkamp et al. (1994) proposed the following approximate expansion for the description
 86 of the steady-state for water infiltrated through a disc source while maintaining a zero water pressure
 87 head at surface:

$$88 \quad I_{3D}^{+\infty}(t) = \left(K_s + \frac{\gamma S^2}{r_d \Delta\theta} \right) t + \frac{S^2}{2(1-\beta)\Delta K} \ln\left(\frac{1}{\beta}\right) \quad (5)$$

89 Where r (L) is the radius of the source, γ and β are two infiltration constants, often fixed at 0.75 and
 90 0.6, respectively (Haverkamp et al., 1994). b_s (L) and i_s ($L T^{-1}$) that are the intercept and slope of the
 91 steady state approximate expansion are defined as a function of hydraulic conductivity and sorptivity
 92 as follows:

$$93 \quad i_s = K_s + \frac{\gamma S^2}{r_d \Delta\theta} \quad (6a)$$

$$94 \quad b_s = \frac{S^2}{2(1-\beta)\Delta K} \ln\left(\frac{1}{\beta}\right) \quad (6b)$$

95 In this study, we use the equation defining the intercept, b_s , to quantify the ratio between sorptivity
 96 and the difference in hydraulic conductivity, as already suggested by Castellini et al. (2018):

$$97 \quad \frac{S^2}{\Delta K} = \frac{b_s}{C} \quad (7a)$$

$$98 \quad C = \frac{1}{2(1-\beta)} \ln\left(\frac{1}{\beta}\right) \quad (7b)$$

99

100 The implementation of such expression into equation (4) leads to the following expression for the
101 macroscopic capillary length:

$$102 \quad \lambda_c = \frac{b}{\Delta\theta} \frac{b_s}{c} \quad (8)$$

103 Eq. (8) constitutes a considerable simplification, allowing to estimate the macroscopic capillary
104 length, λ_c , by only using the infiltration experiment and a measurement of difference between the
105 initial and saturated soil water contents, $\Delta\theta$. Indeed, once the intercept of the steady state, b_s , is
106 estimated, using for instance the linear regression of the last points of the cumulative infiltration, and
107 once the parameter b is determined, λ_c can be easily determined. Note that White and Sully (1987)
108 fixed b at 0.55 for the case when the initial hydraulic conductivity is far lower than the saturated
109 hydraulic conductivity, $K_i \ll K_s$. In addition, β is fixed at 0.6, leading to a value of 0.639.

110 The previous estimation of the macroscopic capillary length may allow the estimation of the
111 saturated hydraulic conductivity. Many methods for calculating the saturated soil hydraulic
112 conductivity from single-ring data require an estimation of λ_c or its inverse α . Thus, in this
113 investigation, we also assessed the impact of the proposed approach on K_s calculation. Among the λ_c -
114 dependent methods, we considered the following methods for estimating the saturated hydraulic
115 conductivity:

- 116 **i)** the One-Ponding Depth (**OPD**) method by Reynolds and Elrick (1990);
- 117 **ii)** the method 2 by Wu et al. (1999) (**WU2**);
- 118 **iii)** the Steady version of the Simplified method based on a Beerkan Infiltration run (**SSBI**) by
119 Bagarello et al. (2017);
- 120 **iv)** the Approach 4 (**A4**) by Stewart and Abou Najm (2018b).

121 All these calculation procedures have been detailed in **Table E**. For this investigation, only steady
122 state methods have been selected because the proposed λ_c estimation procedure is also based on steady
123 state data analysis, thus they all consider the same experimental information. In addition, the late
124 phase of the infiltration process is easier to interpret in comparison to the transient state (Di Prima et

125 al., 2018a), which is frequently subjected to different and sometimes simultaneous perturbations,
 126 especially on water repellent soils or soils with macropores (Angulo-Jaramillo et al., 2019).

127 3. Material and methods

128 3.1. Analytically generated data

129 We assessed the accuracy of the proposed calculation approach to yield reliable λ_c and K_s
 130 predictions by using the same six soils (i.e., sand, loamy sand, sandy loam, loam, silt loam, silty clay
 131 loam) considered by Hinnell et al. (2009) and Bagarello et al. (2017) to cover a wide range of
 132 hydraulic responses. We modelled the infiltration experiments for these synthetic soils using the
 133 parameters listed by Carsel and Parrish (1988) to describe the water retention curve and the hydraulic
 134 conductivity function according to the van Genuchten–Mualem model (Mualem, 1976; van
 135 Genuchten, 1980) (**Table C**):

$$136 \quad \begin{cases} \theta(h) = \theta_r + (\theta_s - \theta_r)[1 + \alpha_{VG}|h|^n]^{-m} & h < 0 \\ \theta(h) = \theta_s & h \geq 0 \end{cases} \quad (9a)$$

$$137 \quad m = 1 - \frac{1}{n} \quad (9b)$$

$$138 \quad K(h) = \hat{K}_s Se^l [1 - (1 - Se^{1/m})^m]^2 \quad (9c)$$

139 where \hat{K}_s ($L T^{-1}$) is the actual value of the saturated soil hydraulic conductivity, α_{VG} is an empirical
 140 parameter related to the inverse of the air-entry pressure head, n is the pore size distribution index, Se
 141 $= (\theta - \theta_r)/(\theta_s - \theta_r)$ is the effective saturation degree, θ_r ($L^3 L^{-3}$) is the residual water content, l is the
 142 pore connectivity parameter, assumed to be 0.5 by Mualem (1976). To also test the effect of the initial
 143 soil water content on parameters predictions, initial values of Se ranging from 0.1 to 0.8 were
 144 considered when modeling infiltration. For a given soil and an initial Se value, the actual value of the
 145 macroscopic capillary length, $\hat{\lambda}_c$, was estimated by Eq. (2).

146 The cumulative infiltration curves were generated using the infiltration model proposed by
 147 Haverkamp et al. (1994). More specifically, for any zero or negative value of the pressure head at the

148 soil surface, 1D cumulative infiltration, I_{1D} (L), into an initially uniform unsaturated soil profile can
 149 be modelled by the following 1D implicit equation (Haverkamp et al., 1990):

$$150 \quad \frac{2\Delta K^2}{S^2} t = \frac{1}{1-\beta} \left[\frac{2\Delta K}{S^2} (I_{1D}(t) - K_i t) - \ln \left(\frac{\exp\left(2\beta \frac{\Delta K}{S^2} (I_{1D}(t) - K_i t)\right) + \beta - 1}{\beta} \right) \right] \quad (10)$$

151 with $\Delta K = \widehat{K}_s - K_i$. Eq. (10) was extended to three-dimensional (3D) infiltration from a surface
 152 disk source by Smettem et al. (1994), adding a term representing 3D geometrical effects [see Eq. (23)
 153 of Smettem et al., 1994]:

$$154 \quad I(t) = I_{1D}(t) + \frac{\gamma S^2}{r_d \Delta \theta} \quad (11)$$

155 where I is 3D cumulative infiltration, γ is a shape parameter for geometrical correction of the
 156 infiltration front shape, commonly set at 0.75 for $\theta_i < 0.25 \theta_s$ (Haverkamp et al., 1994). For a given
 157 soil and an initial Se value, sorptivity was estimated from soil hydraulic properties in the interval of
 158 soil water pressure head between h_i and 0 as follows (Parlange, 1975):

$$159 \quad S = \sqrt{\int_{h_i}^0 (\theta_s + \theta - 2\theta_i) K(h) dh} \quad (12)$$

160 Then, Eqs. (10) and (11) were used to generate cumulative infiltration curves. Shape parameters β
 161 and γ were assumed equal to the default values, i.e., 0.6 and 0.75, respectively (Angulo-Jaramillo et
 162 al., 2019). The duration of the infiltration process was fixed at three times the maximum time, t_{max}
 163 (T), for which the transient expression of the 3D Haverkamp equation (see Eq. (3a) in Lassabatere et
 164 al. 2006) can be considered valid, with t_{max} calculated as follows (Lassabatere et al., 2006):

$$165 \quad t_{max} = \frac{1}{4(1-B)^2} \left(\frac{S}{\widehat{K}_s} \right)^2 \quad (13a)$$

$$166 \quad B = \frac{2-\beta}{3} \left(1 - \frac{K_i}{\widehat{K}_s} \right) + \frac{K_i}{\widehat{K}_s} \quad (13b)$$

167 These analytical data were used to estimate the intercept, b_s , and the slope, i_s , by linear regression
 168 analysis of the last three data points of the cumulative infiltration versus time plot, which were
 169 assumed to provide a reliable description of steady state conditions. Then, we estimated λ_c and K_s by
 170 Eqs. (8) and (t1-4), respectively. These estimates were compared with the corresponding actual

171 values, i.e., the $\hat{\lambda}_c$ values estimated with Eq. (2) and the \hat{K}_s values by Carsel and Parrish (1988) listed
172 in **Table C**, using the relative error, Er , defined as follows:

$$173 \quad Er(x) = 100 \times \frac{x - \hat{x}}{\hat{x}} \quad (14)$$

174 Where \hat{x} is the actual value for $\hat{\lambda}_c$ or \hat{K}_s and x is the corresponding estimated value λ_c or K_s . Note
175 that positive $Er(x)$ values indicate overestimations whereas negative values indicate
176 underestimations. Small deviations, i.e., $Er(x) \sim 0$, suggest that the estimated soil hydraulic
177 parameters are close to actual values. According to the accuracy criterion by Reynolds (2013), the
178 estimates were deemed accurate when they fell within the range $0.75 \leq x / \hat{x} \leq 1.25$ (i.e. $\leq 25\%$ error).
179 Such a stringent accuracy criterion was used because the parameters were estimated by analytically
180 generated data, and therefore they were free of the perturbations embedded in field and laboratory
181 measurements (e.g., measurement error, random noise and natural variability).

182 **3.2. The Beerkan infiltration database**

183 In this investigation we considered a large database of Beerkan infiltration experiments carried out
184 in four different countries, i.e., Italy, Burundi, France and Spain, during the period 2010-2017 (**Table**
185 **S**). However, nearly half of the runs, i.e., the 46.7% were carried out in Sicily (Italy) (202 out of 433).
186 While, the 35,1% of the runs (152 out of 433) were carried out in Burundi in the African great lakes
187 region. The runs were carried out at 433 sampling points on soils having contrasting textural
188 characteristics, i.e., from sandy to clayey (**Figure T**).

189 All Beerkan experiments were carried out according to the methodology described by Lassabatere
190 et al. (2006). As prescribed by the Beerkan method, a stainless steel ring was inserted shallowly into
191 the soil (~ 1 cm). For each run, different volumes of water were successively poured on the confined
192 soil surface. The number of poured volumes varied depending on time needed to reach steady state,
193 as required by the Beerkan method (Angulo-Jaramillo et al., 2019). The Beerkan experiments
194 considered in this investigation were performed using rings with inner diameters from 5 to 30 cm.
195 The volume of water for each pouring was chosen in order to establish ponding condition on the entire

196 infiltration surface; the volumes ranged from 17 to 800 mL, depending on the used ring (**Table S**).
197 The energy of the falling water was dissipated with fingers to minimize the soil disturbance owing to
198 water pouring, as commonly suggested (e.g., Di Prima et al., 2019). For each poured volume, the time
199 needed for the water to infiltrate was recorded, and the cumulative infiltration, I (mm), was plotted
200 against time, t (h).

201 Similarly to the procedure previously described to analyse analytical generated curves, for each
202 Beerkan experiment we estimated the intercept, b_s (mm), and the slope, i_s (mm h⁻¹), of the regression
203 line fitted to the data points describing steady state conditions. Then, we estimated λ_c and K_s by Eqs.
204 (8) and (t1-4), respectively.

205 For the field data, we chose not to use a reference λ_c value, as an independent datum that can be
206 used for assessing simplified procedures or validating new developed methods does not currently
207 exist. In addition, methods for estimating λ_c from single-ring infiltration experiments are based on
208 cumbersome field procedures.

209 According to Elrick and Reynolds (1992), we classified the λ_c estimates in five soil capillarity
210 categories, i.e., from negligible ($\lambda_c \leq 10$ mm) to very strong ($\lambda_c \geq 1000$ mm) (**Table L**). Note that
211 these categories were originally proposed to select a representative value of the sorptive number, α
212 (L⁻¹), which is equal to λ_c^{-1} , on the basis of five soil texture-structure categories when calculating K_s
213 by the OPD method (Angulo-Jaramillo et al., 2016). In this investigation, we also propose range
214 values for each category as detailed in **Table L**.

215 For K_s , we used as a benchmark the values obtained with the BEST-steady method proposed by
216 Bagarello et al. (2014c), which estimates K_s as follows:

$$217 \quad K_{s,BEST} = \frac{C i_s}{A b_s + C} \quad (15a)$$

$$218 \quad A = \frac{\gamma}{r(\theta_s - \theta_i)} \quad (15b)$$

219 Thus, the K_s values estimated by Eqs. (t1-4) were compared with those obtained by Eq. (15) in terms
220 of relative errors using Eq. (14). We chose this method, as it involves the same experimental

221 information of the λ_c -dependent methods considered in this investigation for estimating K_s , but it does
222 not require an estimation of λ_c .

223 We avoided to use laboratory measurements as benchmark, as they can induce experimental
224 artifacts (Haverkamp et al., 1999), such as soil compaction and samples biased by pores, that may
225 limit their comparability with in-situ measurements (e.g., Bagarello et al., 2009; Di Prima et al.,
226 2018c). Discrepancies are also expected when different measurement techniques are applied in the
227 field or even when the same dataset is analyzed by alternative calculation approaches (Mertens et al.,
228 2002), though in the latter case the results can still be compared to one another (Wu et al., 1999).

229 For comparisons between paired observations, the paired differences, i.e., $K_s - K_{s,BEST}$ for given
230 method, were calculated and the hypothesis of normality of these differences was checked by the
231 Kolmogorov-Smirnov test. For non-normally distributed data the Wilcoxon signed rank test was used
232 to test the median difference between paired observations at $P < 0.05$.

233 4. Results

234 4.1. Analytical validation

235 4.1.1. Actual values of the macroscopic capillary length

236 As expected, Eq. (2) yielded higher $\hat{\lambda}_c$ values for fine-textured soils and lower Se values (**Table**
237 **P**). This is logical, since for fine soils the capillary contribution to water flow was higher than for
238 coarser soils. More specifically, high λ_c values are associated to initially flat $K(h)$ relationships, i.e.,
239 when a decrease in pressure head determines a moderate pore emptying (Angulo-Jaramillo et al.,
240 2016; Reynolds, 1994). As an example, this behavior can be observed on the hydraulic conductivity
241 function of the silty clay loam soil (**Figure K**), where the functional relationship between K and Se
242 is very flat for low Se values, i.e. high pressure head. On the other hand, low λ_c values are associated
243 to steep relationships, i.e., when a small decrease in pressure head determines a more relevant pore
244 emptying (e.g., sand, **Figure K**).

4.1.2. Estimating λ_c from analytically generated data

Cumulative infiltration could be calculated for all cases through Eqs. (10) and (11) and using the parameters listed in Table C. All curves exhibited usual shapes, with a concave shape as a function of time, due to a decreasing hydraulic gradient as the wetting front moves away from the source and the influence of capillarity decreases (Xu et al., 2012). As the process approaches steady state, cumulative infiltration curves become approximately linear with time (Angulo-Jaramillo et al., 2016) (Figure H). Note that the duration of the infiltration process decreased for higher values of the initial effective saturation degree. Indeed, for wetter initial conditions steady state was reached more quickly and with less water (Di Prima et al., 2016). In this case, the influence of capillary forces on infiltration was very short, and the cumulative infiltration curves exhibited a more linear shape (Angulo-Jaramillo et al., 2019).

The values of the intercept, b_s , estimated from these curves, were used in conjunction with the θ_i and θ_s values to calculate λ_c by Eq. (8) (Table P). Then, the λ_c values were compared with the corresponding actual values, $\hat{\lambda}_c$, in terms of relative errors (Figure G). All λ_c values were accurate according to the chosen criterion, since $Er(\lambda_c)$ ranged from -23.2 to 7.9%. The higher $|Er(\lambda_c)|$ values were obtained for the coarse-textured soils, namely the sandy and loamy sand soils, and only for initial wet conditions (Figure G). Under these conditions, the ratio K_i / K_s departed from the assumption made to approximate Eq. (7a) (i.e., $K_i \ll K_s$). More specifically, near the saturation, the ratio K_i / K_s was higher for the coarser soils than for the fine-textured soils because the capillary forces were weaker and the increase of the hydraulic conductivity near the saturation was less abrupt (Figure K). As a consequence, for the coarser soils, neglecting the K_i / K_s ratio in Eq. (7a) negatively affected λ_c estimates, yielding higher errors. Nevertheless, λ_c estimates were sufficiently accurate also in these cases, with errors always lower than 25%.

268 4.1.3. Estimating K_s from analytically generated data

269 The values of the slope, i_s , estimated from the analytically generated curve, were used to calculate
270 K_s by the four λ_c -dependent methods (i.e., OPD, WU2, SSBI, A4) using Eqs. (t1-4) (Table P). Then,
271 the K_s values were compared with the corresponding actual values, \hat{K}_s (Table C), in terms of relative
272 errors (Figure W). The $Er(K_s)$ values ranged from -3.1 to 9.5%, from -7.4 to 5.4%, from -24.7 to -
273 2.2%, and from 2.4 to 14%, for the OPD, WU2, SSBI and A4 methods, respectively. Mean $|Er(K_s)|$
274 values were ordered as OPD < A4 < WU2 < SSBI. Therefore, the OPD method was the most accurate
275 overall. However, the four methods always yielded accurate estimates, since $|Er(K_s)|$ values were
276 always lower than 25% (Figure W).

277 4.2. Field testing

278 4.2.1. Peculiarities and experiments exclusion

279 For six Beerkan experiments infiltration rates increased with time, such that the cumulative
280 infiltration curves exhibited convex shapes. The cumulative infiltration data in that instance yielded
281 a negative value for the intercept, b_s . This circumstance led to negative λ_c data. In addition, in case of
282 negative intercept values, the BEST-steady algorithm is also expected to estimate meaningless K_s
283 data (Angulo-Jaramillo et al., 2019). For this reason these Beerkan experiments were excluded from
284 subsequent analyses. These cases occurred at the Kinyami site (two instances), Palermo - SAAF site
285 (one instance) and Crépieux-Charmy site (three instances), and reflect that the early wetting phase
286 was impeded due to soil water repellency (Concialdi et al., 2019). Hydrophobia may be attributed to
287 locally high OC content (Goebel et al., 2011), exudates produced by the plant root systems or living
288 organisms like arbuscular mycorrhizal fungi (Rillig et al., 2010), and organic pollutants such as
289 hydrocarbons (Durand et al., 2005).

290 4.2.2. Estimating λ_c from the Beerkan infiltration database

291 The Beerkan experiments that were not affected by flow impedance (427 out of 433) could be
292 analyzed to determine λ_c . Eq. (8) yielded λ_c values ranging from 1.5 to 737.7 mm (Table Q).

293 According to the soil capillarity categories suggested by Elrick and Reynolds (1992), the λ_c values
294 were classified as representative of strong capillarity conditions in 29.7% of the cases (127 out of
295 427), moderate in the 44.3% (189), weak in the 25.1% (107), and negligible in the 0.9% (4) (**Figure**
296 **D**). The categories weak and negligible were associated with the higher sand contents, i.e., 35% and
297 37%, respectively. Thus, for the field experiments, Eq. (3) estimated the lowest λ_c values for the
298 coarsest soils, i.e., when gravity was expected to prevail over capillarity. This result increases our
299 confidence on the proposed calculation approach.

300 Three different examples of λ_c estimation are shown in **Figure Fb-d**. The cases differs by the
301 regime of the infiltration process and the shape of the cumulative infiltration. More specifically, we
302 considered: i) an infiltration process that is initially capillary driven and then, at the late phase, both
303 capillary and gravity driven (first case, **Figure Fb**), ii) an infiltration processes dominated by
304 capillarity (second case, **Figure Fc**), and an infiltration processes dominated by gravity (third case,
305 **Figure Fd**). According to Angulo-Jaramillo et al. (2019), these cases correspond to three typical
306 responses when applying the Beerkan protocol respectively on i) regular soils, ii) very fine soils and
307 iii) very coarse soils (see their Figure 13).

308 In the first case (**Figure Fb**), cumulative infiltration exhibits an usual concave shape as a function
309 of time. For this run, we estimated an intercept value of 30.9 mm, and a λ_c value of 49.2 mm falling
310 within the range of $42 \leq \lambda_c \leq 125$ mm (**Figure Fa**). According to the capillarity categories suggested
311 by Elrick and Reynolds (1992), the estimated λ_c value is representative of moderate capillarity
312 conditions (**Table L**).

313 In the second case (**Figure Fc**), the cumulative infiltration curve exhibits a strong concave shape
314 with an intercept value of 209.6 mm, yielding a λ_c value of 598.7 mm, falling within the strong
315 capillary category (**Table L** and **Figure Fa**). This behavior is typical for very fine soils, with low
316 permeability. For this run, capillary forces predominates for almost the duration of the experiment
317 and the attainment of steady state required more time (Di Prima et al., 2016).

318 In the third case (**Figure Fd**), the cumulative infiltration curve exhibits an almost linear shape with
319 an intercept value of 1.0 mm, yielding a λ_c value of 1.5 mm, i.e., lower than the considered threshold
320 of 10 mm for negligible capillarity forces (**Table L** and **Figure Fa**). This behaviour is typical for
321 coarse-textured soils and occurs when the infiltration process is mainly driven by gravity. Negligible
322 values of λ_c were also reported in other investigations (e.g., Khaleel and Relyea, 2001; Russo et al.,
323 1997; White and Sully, 1992). In this investigation we obtained negligible λ_c values in only four cases
324 out of 427. These cases corresponded to the lowest measured intercept values (**Figure Fa**).

325 **4.2.3. Estimating K_s from the Beerkan infiltration database**

326 The differences between K_s and $K_{s,BEST}$ were always non-normally distributed according to the
327 Kolmogorov-Smirnov test. The Wilcoxon signed rank test showed that the four methods (i.e., OPD,
328 WU2, SSBI, A4) yielded K_s estimates significantly different from the BEST-steady values. However,
329 the discrepancies between methods were always lower than $\leq 25\%$, with the exception of the SSBI
330 method (**Figure Z**). More specifically, the method that yielded the lowest discrepancies was the WU2
331 method. This method yielded K_s values ranging from 1.4 to 3493.8 mm h⁻¹ (**Table Q**), with 76 and
332 24% of the runs yielding respectively lower and higher K_s estimates than the BEST-estimated values
333 (**Figure Z**). The median K_s values differed by only a factor of 1.002. The relative error, $Er(K_s)$, ranged
334 from -12.1 to 22.1%. Therefore, according to selected criterion (i.e., discrepancies $\leq 25\%$), the WU2
335 and BEST-steady methods yielded similar K_s estimates. The OPD and A4 methods also gave $|Er(K_s)|$
336 values always lower than 25%, suggesting that also these methods yielded similar K_s estimates to
337 those values obtained by BEST-steady. Larger discrepancies were only obtained when using the SSBI
338 method. This method always yielded K_s values higher than $K_{s,BEST}$, with only one exception. The
339 $Er(K_s)$ values ranged from -1.0 to 32.8%, with 21% of the runs (88 out of 427) yielding higher values
340 than the considered threshold of 25%.

341 5. Discussion

342 In this investigation, we proposed to estimate the macroscopic capillary length using a simple
343 Beerkan infiltration experiment and a measurement of the initial and saturated soil water contents.
344 Previous investigations also suggested that the measured infiltration curve contains the necessary
345 information to estimate λ_c (Bagarello et al., 2013, e.g., 2014d; Stewart and Abou Najm, 2018a; Wu
346 et al., 1999). However, these methods are based on the analysis of the transient infiltration process.
347 Indeed, they all require an estimation of the infiltration coefficients by the fitting of transient models
348 to early infiltration data. It is not uncommon that these methods perform poorly, especially in case of
349 uncertainties on the transient phase (e.g., Di Prima et al., 2019, 2018b). While these methods may
350 alleviate the experimental efforts needed to determine λ_c and K_s in the field, for instance, reducing
351 the required measurement time for low permeability soils (Bagarello et al., 2014d), they may
352 introduce uncertainties on the hydraulic characterization and increase parameter variability (Di Prima
353 et al., 2018b). This limitation can ultimately complicate an accurate assessment of spatial-temporal
354 variability of soil hydraulic properties (Angulo-Jaramillo et al., 2016).

355 On the other hand, the proposed method uses the experimental information collected during the
356 final stage of the infiltration process, thus, it is expected to be less sensitive to experimental data
357 accuracy (Bagarello et al., 2013). Estimating λ_c requires the intercept (b_s) that can be easily calculated
358 by linear regression analysis of the final portion of the cumulative infiltration. While the final
359 infiltration rate (i_s) is totally independent from the early phase of the infiltration process, the intercept
360 depends on the shape of the cumulative infiltration curve, thus, it restitutes a certain information on
361 the transient phase (Bagarello et al., 2014c). The shape of the cumulative infiltration, in turn, reveals
362 the relative importance of capillary and gravity forces during a ponding infiltration process, being
363 more concave or linear respectively in case of prevalence of capillarity over gravity or vice versa
364 (Angulo-Jaramillo et al., 2019). More specifically, small values of the intercept are indicative of a
365 linear infiltration curve, i.e., when gravity prevails over capillarity, which occurs primarily in coarse-
366 textured and/or highly structured porous media. On the contrary, high intercept values are indicative

367 of a concave infiltration curve, i.e., when capillarity prevails over gravity, which occurs primarily in
368 fine-textured soils. Therefore, b_s is expected to be a reliable predictor of the macroscopic capillary
369 length.

370 In this investigation, this hypothesis was validated by assessing the proposed calculation approach
371 using both analytical and field data. The analytical validation demonstrated that Eq. (8) was able to
372 provide reliable λ_c estimates over a wide range of soil textural characteristics and initial soil water
373 contents. We also tested the new method on a large database including 433 Beerkan infiltration
374 experiments carried out on different soils having contrasting textural characteristics, i.e., from sandy
375 to clayey. The 99.1% of the experiments yielded λ_c values falling within the realistic range
376 $10 \leq \lambda_c \leq 1000$ mm (W. D. Reynolds and Elrick, 2002), with the only expectation of four cases
377 yielding negligible λ_c values, i.e., lower than 10 mm.

378 An expected advantage of the proposed method is to improve K_s prediction since it avoids to
379 choose a λ_c value on the basis of the soil capillarity categories. Indeed, using Eqs. (t1-4) needs
380 knowledge of λ_c , that, according to Elrick and Reynolds (1992), can be estimated on the basis of a
381 general description of soil textural and structural characteristics (**Table L**). The effect of an erroneous
382 choice of the capillarity category on K_s predictions was investigated by Bagarello et al. (2014d). These
383 authors assessed the sensitivity of K_s to the right choice of the capillarity category, reporting that an
384 erroneous choice of the capillarity category, for instance differing by plus or minus one category from
385 the correct one, may also lead to discrepancies between K_s estimates of more than a factor of three.
386 A sensitivity analysis to determine the effect of errors in constraining λ_c on K_s estimations was also
387 performed by Stewart and Abou Najm (2018b). These authors reported that K_s estimates are more
388 sensitive to underpredictions of λ_c compared with overpredictions. Therefore, choosing an erroneous
389 λ_c value from the previous capillarity category may have a more relevant effect than choosing the λ_c
390 value from the successive category. In any case, the subjectivity on the choice of an appropriate λ_c
391 value constitutes a clear limitation when using λ_c -dependent methods for estimating K_s , such as those

392 considered in this investigation. On the contrary, the proposed method avoids any subjectivity on the
393 estimation of λ_c .

394 A possible limitation when using this calculation approach, especially on very fine soils, is related
395 to the need of infiltrating enough water during the experiment in order to approach steady state
396 conditions. Indeed, fine-textured and unstructured soils often exhibit very low permeability, thus, the
397 attainment of steady state may require excessively long experiments (Di Prima et al., 2016), which
398 would complicate reaching steady state conditions with the regular Beerkan protocol (Alagna et al.,
399 2016a). This problem can be easily solved using automated devices, such as the one developed by Di
400 Prima (2015) and Concialdi et al. (2019), that allows accurate and automated infiltration rates
401 measurements. The first obvious advantage in using automatic infiltrometer in case of low
402 permeability soils is that data collection is automated and it does not require any further manipulation
403 by the user once the device is installed. Therefore, tests can be simultaneously performed alleviating
404 the experimental efforts in case of long experiments durations (Alagna et al., 2018).

405 **6. Summary and conclusions**

406 In this investigation, we assessed a simple field method for estimating the macroscopic capillary
407 length, λ_c , by only using a single-ring infiltration experiment of the Beerkan type and a measurement
408 of the initial and saturated soil water contents. We validated the proposed method by using both
409 analytical generated data and a large database of 433 Beerkan infiltration experiments carried out in
410 four different countries, i.e., Italy, Burundi, France and Spain, during the period 2010-2017. While
411 the analytical validation supported our hypothesis that the intercept, b_s , is a reliable predictor of the
412 macroscopic capillary length, the testing carried out using the Beerkan database increased our
413 confidence on the proposed calculation approach. This method constitutes an easy solution to estimate
414 λ_c , and it can be applied in conjunction with a number of λ_c -dependent methods for estimating the
415 saturated soil hydraulic conductivity, allowing to improve K_s prediction in the field. The proposed

416 method may also avoid any subjectivity caused by the selection of a representative λ_c value on the
417 only base of textural and structural characteristics.

418 **Funding:** This work was supported through the INFILTRON Project (ANR-17-CE04-0010, Package
419 for assessing infiltration & filtration functions of urban soils in stormwater management;
420 <https://infiltron.org/>) funded by the French National Research Agency (ANR), and the “Programma
421 Operativo Nazionale (PON) Ricerca e Innovazione 2014-2020 (Linea 1 - Mobilità dei ricercatori,
422 AIM1853149, CUP: J54I18000120001) funded by the European Regional Development Fund
423 (ERDF) and the Italian Ministry of Education, University and Research (MIUR).

424 **Author Contributions:** S. Di Prima outlined the investigation, developed the theory and analyzed
425 the data. All authors contributed to discussing the results and writing the manuscript.

426 **Conflicts of Interest:** The authors declare no conflict of interest.

427 **References**

- 428 Alagna, V., Bagarello, V., Di Prima, S., Giordano, G., Iovino, M., 2016a. Testing infiltration run effects on
429 the estimated water transmission properties of a sandy-loam soil. *Geoderma* 267, 24–33.
430 <https://doi.org/10.1016/j.geoderma.2015.12.029>
- 431 Alagna, V., Bagarello, V., Di Prima, S., Iovino, M., 2016b. Determining hydraulic properties of a loam soil
432 by alternative infiltrometer techniques. *Hydrological Processes* 30, 263–275.
433 <https://doi.org/10.1002/hyp.10607>
- 434 Alagna, V., Iovino, M., Bagarello, V., Mataix-Solera, J., Lichner, L., 2018. Alternative analysis of transient
435 infiltration experiment to estimate soil water repellency. *Hydrological Processes*.
436 <https://doi.org/10.1002/hyp.13352>
- 437 Angulo-Jaramillo, R., Bagarello, V., Di Prima, S., Gosset, A., Iovino, M., Lassabatere, L., 2019. Beerkan
438 Estimation of Soil Transfer parameters (BEST) across soils and scales. *Journal of Hydrology* 576,
439 239–261. <https://doi.org/10.1016/j.jhydrol.2019.06.007>
- 440 Angulo-Jaramillo, R., Bagarello, V., Iovino, M., Lassabatère, L., 2016. *Infiltration Measurements for Soil
441 Hydraulic Characterization*. Springer International Publishing.
- 442 Bagarello, V., Castellini, M., Di Prima, S., Giordano, G., Iovino, M., 2013. Testing a Simplified Approach to
443 Determine Field Saturated Soil Hydraulic Conductivity. *Procedia Environmental Sciences* 19, 599–
444 608. <https://doi.org/10.1016/j.proenv.2013.06.068>
- 445 Bagarello, V., Castellini, M., Di Prima, S., Iovino, M., 2014a. Soil hydraulic properties determined by
446 infiltration experiments and different heights of water pouring. *Geoderma* 213, 492–501.
447 <https://doi.org/10.1016/j.geoderma.2013.08.032>
- 448 Bagarello, V., Di Prima, S., Giordano, G., Iovino, M., 2014b. A test of the Beerkan Estimation of Soil
449 Transfer parameters (BEST) procedure. *Geoderma* 221–222, 20–27.
450 <https://doi.org/10.1016/j.geoderma.2014.01.017>

- 451 Bagarello, V., Di Prima, S., Iovino, M., 2017. Estimating saturated soil hydraulic conductivity by the near
452 steady-state phase of a Beerkan infiltration test. *Geoderma* 303, 70–77.
453 <https://doi.org/10.1016/j.geoderma.2017.04.030>
- 454 Bagarello, V., Di Prima, S., Iovino, M., 2014c. Comparing Alternative Algorithms to Analyze the Beerkan
455 Infiltration Experiment. *Soil Science Society of America Journal* 78, 724.
456 <https://doi.org/10.2136/sssaj2013.06.0231>
- 457 Bagarello, V., Di Prima, S., Iovino, M., Provenzano, G., 2014d. Estimating field-saturated soil hydraulic
458 conductivity by a simplified Beerkan infiltration experiment. *Hydrological Processes* 28, 1095–1103.
459 <https://doi.org/10.1002/hyp.9649>
- 460 Bagarello, V., Di Prima, S., Iovino, M., Provenzano, G., Sgroi, A., 2011. Testing different approaches to
461 characterize Burundian soils by the BEST procedure. *Geoderma* 162, 141–150.
462 <https://doi.org/10.1016/j.geoderma.2011.01.014>
- 463 Bagarello, V., Iovino, M., Elrick, D., 2004. A Simplified Falling-Head Technique for Rapid Determination
464 of Field-Saturated Hydraulic Conductivity. *Soil Science Society of America Journal* 68, 66.
465 <https://doi.org/10.2136/sssaj2004.6600>
- 466 Bagarello, V., Sferlazza, S., Sgroi, A., 2009. Testing laboratory methods to determine the anisotropy of
467 saturated hydraulic conductivity in a sandy-loam soil. *Geoderma* 154, 52–58.
468 <https://doi.org/10.1016/j.geoderma.2009.09.012>
- 469 Bouwer, H., 1964. Unsaturated Flow in Ground-Water Hydraulics. *Journal of the Hydraulics Division* 90,
470 121–144.
- 471 Carsel, R.F., Parrish, R.S., 1988. Developing joint probability distributions of soil water retention
472 characteristics. *Water Resour. Res.* 24, 755–769. <https://doi.org/10.1029/WR024i005p00755>
- 473 Concialdi, P., Di Prima, S., Bhanderi, H.M., Stewart, R.D., Abou Najm, M.R., Gaur, M.L., Angulo-
474 Jaramillo, R., Lassabatere, L., 2019. An open-source instrumentation package for intensive soil
475 hydraulic characterization. Submitted to *Journal of Hydrology*.
- 476 Di Prima, S., 2015. Automated single ring infiltrometer with a low-cost microcontroller circuit. *Computers
477 and Electronics in Agriculture* 118, 390–395. <https://doi.org/10.1016/j.compag.2015.09.022>
- 478 Di Prima, S., Bagarello, V., Lassabatere, L., Angulo-Jaramillo, R., Bautista, I., Burguet, M., Cerdà, A.,
479 Iovino, M., Prosdoci, M., 2017. Comparing Beerkan infiltration tests with rainfall simulation
480 experiments for hydraulic characterization of a sandy-loam soil. *Hydrological Processes* 31, 3520–
481 3532. <https://doi.org/10.1002/hyp.11273>
- 482 Di Prima, S., Castellini, M., Abou Najm, M.R., Stewart, R.D., Angulo-Jaramillo, R., Winiarski, T.,
483 Lassabatere, L., 2019. Experimental assessment of a new comprehensive model for single ring
484 infiltration data. *Journal of Hydrology* 573, 937–951. <https://doi.org/10.1016/j.jhydrol.2019.03.077>
- 485 Di Prima, S., Concialdi, P., Lassabatere, L., Angulo-Jaramillo, R., Pirastru, M., Cerda, A., Keesstra, S.,
486 2018a. Laboratory testing of Beerkan infiltration experiments for assessing the role of soil sealing on
487 water infiltration. *CATENA* 167, 373–384. <https://doi.org/10.1016/j.catena.2018.05.013>
- 488 Di Prima, S., Lassabatere, L., Bagarello, V., Iovino, M., Angulo-Jaramillo, R., 2016. Testing a new
489 automated single ring infiltrometer for Beerkan infiltration experiments. *Geoderma* 262, 20–34.
490 <https://doi.org/10.1016/j.geoderma.2015.08.006>
- 491 Di Prima, S., Lassabatere, L., Rodrigo-Comino, J., Marrosu, R., Pulido, M., Angulo-Jaramillo, R., Úbeda,
492 X., Keesstra, S., Cerdà, A., Pirastru, M., 2018b. Comparing Transient and Steady-State Analysis of
493 Single-Ring Infiltration Data for an Abandoned Field Affected by Fire in Eastern Spain. *Water* 10.
494 <https://doi.org/10.3390/w10040514>
- 495 Di Prima, S., Marrosu, R., Lassabatere, L., Angulo-Jaramillo, R., Pirastru, M., 2018c. In situ characterization
496 of preferential flow by combining plot- and point-scale infiltration experiments on a hillslope.
497 *Journal of Hydrology* 563, 633–642. <https://doi.org/10.1016/j.jhydrol.2018.06.033>
- 498 Durand, C., Ruban, V., Amblès, A., 2005. Characterisation of complex organic matter present in
499 contaminated sediments from water retention ponds. *Journal of Analytical and Applied Pyrolysis* 73,
500 17–28. <https://doi.org/10.1016/j.jaap.2004.09.001>
- 501 Elrick, D.E., Reynolds, W.D., 1992. Methods for analyzing constant-head well permeameter data. *Soil
502 Science Society of America Journal* 56, 320.
503 <https://doi.org/10.2136/sssaj1992.03615995005600010052x>
- 504 Gardner, W., 1958. Some steady-state solutions of the unsaturated moisture flow equation with application to
505 evaporation from a water table. *Soil science* 85, 228–232.

506 Goebel, M.-O., Bachmann, J., Reichstein, M., Janssens, I.A., Guggenberger, G., 2011. Soil water repellency
507 and its implications for organic matter decomposition – is there a link to extreme climatic events?
508 *Global Change Biology* 17, 2640–2656. <https://doi.org/10.1111/j.1365-2486.2011.02414.x>
509 Haverkamp, R., Bouraoui, F., Zammit, C., Angulo-Jaramillo, R., 1999. Soil properties and moisture
510 movement in the unsaturated zone. *Handbook of groundwater engineering*.
511 Haverkamp, R., Parlange, J.-Y., Starr, J., Schmitz, G., Fuentes, C., 1990. Infiltration under ponded
512 conditions: 3. A predictive equation based on physical parameters. *Soil science* 149, 292–300.
513 <https://doi.org/10.1097/00010694-199005000-00006>
514 Haverkamp, R., Ross, P.J., Smettem, K.R.J., Parlange, J.Y., 1994. Three-dimensional analysis of infiltration
515 from the disc infiltrometer: 2. Physically based infiltration equation. *Water Resour. Res.* 30, 2931–
516 2935. <https://doi.org/10.1029/94WR01788>
517 Hinnell, A.C., Lazarovitch, N., Warrick, A.W., 2009. Explicit infiltration function for boreholes under
518 constant head conditions: INFILTRATION FUNCTION FOR BOREHOLES. *Water Resources*
519 *Research* 45, n/a-n/a. <https://doi.org/10.1029/2008WR007685>
520 Khaleel, R., Relyea, J.F., 2001. Variability of Gardner’s α for coarse-textured sediments. *Water Resources*
521 *Research* 37, 1567–1575. <https://doi.org/10.1029/2000WR900398>
522 Lassabatere, L., Angulo-Jaramillo, R., Soria Ugalde, J.M., Cuenca, R., Braud, I., Haverkamp, R., 2006.
523 Beerkan estimation of soil transfer parameters through infiltration experiments—BEST. *Soil Science*
524 *Society of America Journal* 70, 521. <https://doi.org/10.2136/sssaj2005.0026>
525 Mertens, J., Jacques, D., Vanderborght, J., Feyen, J., 2002. Characterisation of the field-saturated hydraulic
526 conductivity on a hillslope: in situ single ring pressure infiltrometer measurements. *Journal of*
527 *Hydrology* 263, 217–229. [https://doi.org/10.1016/S0022-1694\(02\)00052-5](https://doi.org/10.1016/S0022-1694(02)00052-5)
528 Mualem, Y., 1976. A new model for predicting the hydraulic conductivity of unsaturated porous media.
529 *Water Resour. Res* 12, 513–522.
530 Nimmo, J.R., Schmidt, K.M., Perkins, K.S., Stock, J.D., 2009. Rapid Measurement of Field-Saturated
531 Hydraulic Conductivity for Areal Characterization. *Vadose Zone Journal* 8, 142.
532 <https://doi.org/10.2136/vzj2007.0159>
533 Parlange, J.-Y., 1975. Convergence and validity of time expansion solutions: a comparison to exact and
534 approximate solutions. *Soil Science Society of America Journal* 39, 3–6.
535 Philip, J., 1957. The theory of infiltration: 4. Sorptivity and algebraic infiltration equations. *Soil sci* 84, 257–
536 264.
537 Philip, J.R., 1985. Reply To “Comments on Steady Infiltration from Spherical Cavities.” *Soil Science*
538 *Society of America Journal* 49, 788–789.
539 <https://doi.org/10.2136/sssaj1985.03615995004900030055x>
540 Philip, J.R., 1968. Steady Infiltration From Buried Point Sources and Spherical Cavities. *Water Resources*
541 *Research* 4, 1039–1047. <https://doi.org/10.1029/WR004i005p01039>
542 Raats, P.A.C., 1976. Analytical Solutions of a Simplified Flow Equation. *Transactions of the ASAE* 19,
543 0683–0689. <https://doi.org/10.13031/2013.36096>
544 Reynolds, W., Elrick, D., 2002. 3.4.3.2.b Pressure infiltrometer. In *Methods of Soil Analysis, Part 4,*
545 *Physical Methods*, Dane JH, Topp GC (eds). SSSA Book Series, No. 5. Soil Sci. Soc. Am.:
546 Madison, Wisconsin, USA 4, 826–836.
547 Reynolds, W., Elrick, D., Youngs, E., 2002. 3.4.3.2 Ring or cylinder infiltrometers (vadose zone). In
548 *Methods of Soil Analysis, Part 4, Physical Methods*, Dane JH, Topp GC (eds). SSSA Book Series,
549 No. 5. Soil Sci. Soc. Am.: Madison, Wisconsin, USA 818–820.
550 Reynolds, W.D., 2013. An assessment of borehole infiltration analyses for measuring field-saturated
551 hydraulic conductivity in the vadose zone. *Engineering Geology* 159, 119–130.
552 <https://doi.org/10.1016/j.enggeo.2013.02.006>
553 Reynolds, W.D., 1994. Letter to the editor. Comment on “comparison of three methods for assessing soil
554 hydraulic properties” by G. B. Paige and D. Hillel. *Soil Science* 157, 120.
555 Reynolds, W.D., Elrick, D.E., 2002. 3.4.3.3 Constant Head Well Permeameter (Vadose Zone), in: *Methods*
556 *of Soil Analysis: Part 4 Physical Methods*, SSSA Book Series. Soil Science Society of America,
557 Madison, WI, pp. 844–858. <https://doi.org/10.2136/sssabookser5.4.c33>
558 Reynolds, W.D., Elrick, D.E., 1990. Ponded Infiltration From a Single Ring: I. Analysis of Steady Flow. *Soil*
559 *Science Society of America Journal* 54, 1233.
560 <https://doi.org/10.2136/sssaj1990.03615995005400050006x>

561 Rillig, M.C., Mardatin, N.F., Leifheit, E.F., Antunes, P.M., 2010. Mycelium of arbuscular mycorrhizal fungi
562 increases soil water repellency and is sufficient to maintain water-stable soil aggregates. *Soil*
563 *Biology and Biochemistry* 42, 1189–1191. <https://doi.org/10.1016/j.soilbio.2010.03.027>
564 Russo, D., Russo, I., Laufer, A., 1997. On the spatial variability of parameters of the unsaturated hydraulic
565 conductivity. *Water Resources Research* 33, 947–956. <https://doi.org/10.1029/96WR03947>
566 Smettem, K.R.J., Parlange, J.Y., Ross, P.J., Haverkamp, R., 1994. Three-dimensional analysis of infiltration
567 from the disc infiltrometer: 1. A capillary-based theory. *Water Resour. Res.* 30, 2925–2929.
568 <https://doi.org/10.1029/94WR01787>
569 Smith, R.E., Smettem, K.R., Broadbridge, P., 2002. Infiltration theory for hydrologic applications. American
570 Geophysical Union.
571 Stewart, R.D., Abou Najm, M.R., 2018a. A Comprehensive Model for Single Ring Infiltration I: Initial
572 Water Content and Soil Hydraulic Properties. *Soil Science Society of America Journal* 82, 548–557.
573 <https://doi.org/10.2136/sssaj2017.09.0313>
574 Stewart, R.D., Abou Najm, M.R., 2018b. A Comprehensive Model for Single Ring Infiltration II: Estimating
575 Field-Saturated Hydraulic Conductivity. *Soil Science Society of America Journal* 82, 558–567.
576 <https://doi.org/10.2136/sssaj2017.09.0314>
577 van Genuchten, M.T., 1980. A closed-form equation for predicting the hydraulic conductivity of unsaturated
578 soils. *Soil science society of America journal* 44, 892–898.
579 White, I., Sully, M.J., 1992. On the variability and use of the hydraulic conductivity alpha parameter in
580 stochastic treatments of unsaturated flow. *Water Resour. Res.* 28, 209–213.
581 <https://doi.org/10.1029/91WR02198>
582 White, I., Sully, M.J., 1987. Macroscopic and microscopic capillary length and time scales from field
583 infiltration. *Water Resour. Res.* 23, 1514–1522. <https://doi.org/10.1029/WR023i008p01514>
584 Wooding, R.A., 1968. Steady Infiltration from a Shallow Circular Pond. *Water Resour. Res.* 4, 1259–1273.
585 <https://doi.org/10.1029/WR004i006p01259>
586 Wu, L., Pan, L., Mitchell, J., Sanden, B., 1999. Measuring Saturated Hydraulic Conductivity using a
587 Generalized Solution for Single-Ring Infiltrometers. *Soil Science Society of America Journal* 63,
588 788. <https://doi.org/10.2136/sssaj1999.634788x>
589 Xu, X., Lewis, C., Liu, W., Albertson, J.D., Kiely, G., 2012. Analysis of single-ring infiltrometer data for
590 soil hydraulic properties estimation: Comparison of BEST and Wu methods. *Agricultural Water*
591 *Management* 107, 34–41. <https://doi.org/10.1016/j.agwat.2012.01.004>
592

593

594 **Table E.** Relationships for calculating the saturated soil hydraulic conductivity, K_s , by the One-Ponding
 595 Depth (OPD) method, the method 2 by Wu et al. (1999) (WU2), the Steady version of the Simplified
 596 method based on a Beerkan Infiltration run (SSBI), and the Approach 4 (A4).

Relationships			
OPD	WU2	SSBI	A4
$K_s = \frac{\frac{i_s \pi r^2}{\lambda_c} (0.316 \frac{d}{r} + 0.184)}{r (\frac{H}{\lambda_c} + 1) + (0.316 \frac{d}{r} + 0.184) \frac{\pi r^2}{\lambda_c}}$ <p>(t1)</p>	$K_s = \frac{i_s}{0.9084 (\frac{H + \lambda_c}{G^*} + 1)}$ <p>(t2)</p>	$K_s = \frac{i_s}{\frac{\gamma \gamma_w \lambda_c}{r} + 1}$ <p>(t3)</p>	$K_s = \frac{i_s}{(\frac{H + \lambda_c}{G^*} + 1)}$ <p>(t4)</p>
Parameters			
<p>d (L) = ring insertion depth into the soil. $G^* = d + r/2$. H (L) = ponding depth of water. i_s (L T⁻¹) = steady-state infiltration rate estimated from the cumulative infiltration versus time plot. λ_c (L) = macroscopic capillary length. r (L) = ring radius. γ = dimensionless constant set equal to 0.75 and related to the effect of disk curvature and gravity (Smettem et al., 1994). γ_w = dimensionless constant related to the shape of the wetting front (White and Sully, 1987). A value of $\gamma_w = 1.818$ was suggested by Reynolds and Elrick (2002).</p>			

597

598

599 **Table C.** Soil hydraulic parameters for the five studied soils used to model the infiltration experiments. From
600 Carsel and Parrish (1988).

Soil texture	Sand	Loamy Sand	Sandy Loam	Loam	Silt Loam	Silty Clay Loam
θ_r	0.045	0.057	0.065	0.078	0.067	0.089
θ_s	0.43	0.41	0.41	0.43	0.45	0.43
α_{VG} (mm ⁻¹)	0.0145	0.0124	0.0075	0.0036	0.002	0.001
n	2.68	2.28	1.89	1.56	1.41	1.23
\bar{K}_s (mm h ⁻¹)	297.0	145.9	44.2	10.44	4.5	0.7
l	0.5	0.5	0.5	0.5	0.5	0.5

601

602

603 **Table L.** Soil capillarity categories suggested by Elrick and Reynolds (1992), and representative α (mm^{-1}) and
 604 λ_c (mm) values. The suggested range values for the two parameters are also reported.

Soil capillarity category	Representative α (mm^{-1})	Suggested α range values	Representative λ_c (mm)	λ_c range values
Very strong	≤ 0.001		≥ 1000	
Strong	0.004	$0.001 < \alpha < 0.008$	250	$125 < \lambda_c < 1000$
Moderate	0.012	$0.008 \leq \alpha \leq 0.024$	83	$42 \leq \lambda_c \leq 125$
Weak	0.036	$0.024 < \alpha < 0.1$	28	$10 < \lambda_c < 42$
Negligible	≥ 0.1		≤ 10	

605

606

607 **Table S.** Summary of the Beerkan infiltration database. Total number of Beerkan infiltration
 608 experiments, $N_{tot} = 433$.

Country	Site	N	D (cm)	V (mL)	Coordinates	Reference
Burundi	Nyamutobo (Ruyigi)	77	15	150	3°27'50" S, 30°15'40" E	Bagarello et al. (2011)
Burundi	Kinyami (Ngozi)	20	15	150	2°54'30" S, 29°49'06" E	
Italy	Giampilieri	11	15	150	38°48" N, 15°28'26" E	Bagarello et al. (2013)
Italy	Palermo - SAAF† (Sicily)	8	30	800	38°6'25" N, 13°21'6" E	Bagarello et al. (2014b)
Italy	Caccamo (Sicily)	4	30	800	37°52'34" N, 13°38'43" E	
Italy	Corleone (Sicily)	20	30	800	37°48'35" N, 13°17'49" E	
Italy	Sparacia (Sicily)	8	30	800	37°38'11" N, 13°45'50" E	
Italy	Palermo - SAAF (Sicily)	10	8.5	64	38°6'25" N, 13°21'6" E	Bagarello et al. (2014a)
Italy	Sparacia (Sicily)	10	8.5	64	37°38'10" N, 13°45'59" E	
Italy	Palermo - Parco d'Orleans (Sicily)	10	8.5	64	38°6'26" N, 13°20'59" E	
Italy	Villabate (Sicily)	10	8.5	64	38°4'53" N, 13°25'7" E	
Italy	Palermo - SAAF (Sicily)	12	15	200	38°6'25" N, 13°21'6" E	Bagarello et al. (2014c)
Italy	Palermo - SAAF (Sicily)	4	30	800	38°6'25" N, 13°21'6" E	
Italy	Pietranera (Sicily)	4	15	200	37°32'25" N, 13°30'44" E	
Italy	Pietranera (Sicily)	4	30	800	37°32'25" N, 13°30'44" E	
Italy	Caccamo (Sicily)	4	15	200	37°52'34" N, 13°38'43" E	
Italy	Corleone (Sicily)	20	15	200	37°48'35" N, 13°17'49" E	
Italy	Sparacia (Sicily)	8	15	200	37°38'11" N, 13°45'50" E	
Burundi	Nyamutobo (Ruyigi)	75	15	150	3°27'50" S, 30°15'40" E	
Italy	Palermo - Parco d'Orleans (Sicily)	10	15	150	38°6'26" N, 13°20'59" E	Alagna et al. (2016b)
Italy	Palermo - SAAF (Sicily)	10	15	150	38°6'25" N, 13°21'6" E	Di Prima et al. (2016)
Italy	Palermo - Parco d'Orleans (Sicily)	10	15	150	38°6'26" N, 13°20'59" E	
Italy	Sparacia (Sicily)	10	15	150	37°38'10" N, 13°45'59" E	
France	Crépieux-Charmy (Lyon)	9	15	150	45°47'42" N, 4°53'19" E	
Spain	Les Alcusses de Moixent (Valencia)	10	8.5	48	38°48'33" N, 0°49'3" O	Di Prima et al. (2017)
Italy	Palermo - SAAF (Sicily)	5	5	17	38°6'25" N, 13°21'6" E	Di Prima et al. (2018a)
Italy	Palermo - Parco d'Orleans (Sicily)	5	5	17	38°6'26" N, 13°20'59" E	
Italy	Sparacia (Sicily)	5	5	17	37°38'10" N, 13°45'59" E	
Italy	Baratz Lake watershed (Sardinia)	40	8	43	40°41'53" N, 8°14'4" E	Di Prima et al. (2018c)

609 † Department of Agricultural, Food and Forest Sciences (SAAF = Scienze Agrarie, Alimentari e Forestali).
 610 N = Number of Beerkan infiltration experiments; D (cm) = ring diameter; V (mL) = water volume applied with each pouring.
 611
 612

613 **Table P.** Summary of the soil hydraulic properties for the six synthetic soils.

Soil	Se	h_i (mm)	θ_i (m^3m^{-3})	S ($mm\ h^{-0.5}$) (Eq. 12)	ϕ ($mm^2\ h^{-1}$) (Eq. 3)	$\hat{\lambda}_c$ (mm) (Eq. 2)	λ_c (mm) (Eq. 8)	i_s ($mm\ h^{-1}$)	b_s (mm)	K_s ($mm\ h^{-1}$)			
										OPD (Eq. t1)	WU2 (Eq. t2)	SSBI (Eq. t3)	A4 (Eq. t4)
Sand	0.1	269.0	0.083	86.5	11308.6	38.1	37.2	516.7	15.0	304.3	319.1	341.3	289.8
	0.2	174.5	0.122	81.3	11298.6	38.0	37.0	515.3	13.2	304.2	319.0	341.0	289.7
	0.3	133.1	0.160	75.7	11268.5	37.9	36.8	513.3	11.5	303.7	318.5	340.3	289.3
	0.4	107.8	0.199	69.6	11202.4	37.7	36.7	510.6	9.8	302.4	317.2	338.8	288.1
	0.5	89.7	0.237	62.9	11076.7	37.3	36.7	506.5	8.2	299.8	314.4	335.9	285.6
	0.6	75.2	0.276	55.5	10854.0	36.5	37.1	500.4	6.6	294.9	309.2	330.7	280.9
	0.7	62.5	0.314	46.9	10467.3	35.2	38.2	491.1	5.1	286.1	299.8	321.6	272.3
	0.8	50.2	0.353	36.8	9776.1	32.9	40.5	476.0	3.6	270.3	282.7	305.4	256.8
Loamy Sand	0.1	483.8	0.092	58.2	5602.2	38.4	37.4	254.5	13.8	149.5	156.7	167.8	142.4
	0.2	276.4	0.128	54.7	5598.0	38.4	37.2	253.8	12.2	149.5	156.7	167.6	142.4
	0.3	195.6	0.163	50.9	5584.2	38.3	36.9	252.8	10.6	149.3	156.6	167.4	142.3
	0.4	150.0	0.198	46.8	5552.5	38.1	36.6	251.4	9.0	149.0	156.2	166.9	141.9
	0.5	119.2	0.233	42.3	5490.2	37.6	36.4	249.3	7.5	148.1	155.4	165.8	141.2
	0.6	95.9	0.269	37.3	5376.9	36.9	36.3	246.1	6.0	146.4	153.6	163.9	139.5
	0.7	76.5	0.304	31.5	5176.0	35.5	36.5	241.3	4.5	143.2	150.2	160.4	136.5
	0.8	58.9	0.339	24.6	4811.2	33.0	37.4	233.4	3.1	137.2	143.8	153.9	130.6
Sandy Loam	0.1	1765.2	0.100	36.0	2145.5	49.7	48.3	86.5	17.4	45.4	47.2	52.1	42.9
	0.2	799.2	0.134	33.8	2145.5	49.7	48.0	86.3	15.4	45.4	47.2	52.0	42.9
	0.3	494.2	0.169	31.5	2140.3	49.5	47.6	85.9	13.4	45.4	47.2	52.0	42.9
	0.4	344.1	0.203	29.0	2129.8	49.3	47.1	85.3	11.3	45.3	47.2	51.8	42.9
	0.5	253.1	0.238	26.2	2107.9	48.8	46.5	84.5	9.3	45.2	47.0	51.6	42.7
	0.6	190.3	0.272	23.1	2066.0	47.8	45.7	83.3	7.3	44.8	46.7	51.2	42.5
	0.7	142.4	0.307	19.5	1988.8	46.0	44.9	81.4	5.4	44.2	46.1	50.3	41.8
	0.8	102.3	0.341	15.2	1843.8	42.7	44.0	78.1	3.5	42.8	44.6	48.7	40.6
Loam	0.1	16941.8	0.113	20.9	719.7	69.2	67.6	24.3	24.9	10.7	11.0	12.6	10.0
	0.2	4883.1	0.148	19.6	719.6	69.2	67.2	24.2	22.0	10.7	11.0	12.6	10.0
	0.3	2330.8	0.184	18.3	718.8	69.1	66.6	24.1	19.1	10.7	11.0	12.6	10.0
	0.4	1354.4	0.219	16.8	716.5	68.9	65.9	23.9	16.2	10.7	11.0	12.6	10.0
	0.5	866.2	0.254	15.2	711.0	68.4	64.8	23.7	13.2	10.7	11.0	12.6	10.0
	0.6	579.6	0.289	13.4	699.3	67.2	63.2	23.3	10.3	10.7	11.0	12.5	10.0
	0.7	390.5	0.324	11.3	676.0	65.0	61.0	22.7	7.5	10.6	10.9	12.4	9.9
	0.8	252.5	0.360	8.8	629.2	60.5	57.7	21.6	4.7	10.4	10.8	12.1	9.8
Silt Loam	0.1	1.4×10^5	0.105	16.3	402.8	89.5	87.8	12.3	35.1	4.6	4.7	5.6	4.3
	0.2	25267.3	0.144	15.3	402.8	89.5	87.3	12.2	31.1	4.6	4.7	5.6	4.3
	0.3	9318.5	0.182	14.3	402.6	89.5	86.6	12.2	27.0	4.6	4.7	5.6	4.3
	0.4	4529.8	0.220	13.2	401.8	89.3	85.7	12.1	22.9	4.6	4.7	5.6	4.3
	0.5	2531.6	0.258	11.9	399.6	88.8	84.4	12.0	18.8	4.6	4.7	5.6	4.3
	0.6	1519.5	0.297	10.5	394.4	87.6	82.4	11.8	14.7	4.6	4.7	5.6	4.3
	0.7	933.0	0.335	8.9	383.2	85.2	79.3	11.5	10.6	4.6	4.7	5.5	4.3
	0.8	553.5	0.373	7.0	359.1	79.8	74.2	10.9	6.6	4.6	4.7	5.4	4.3
Silty Clay Loam	0.1	2.2×10^7	0.123	6.0	60.0	85.7	84.9	1.9	30.3	0.7	0.7	0.9	0.7
	0.2	1.1×10^6	0.157	5.6	60.0	85.7	84.5	1.9	26.8	0.7	0.7	0.9	0.7
	0.3	1.9×10^5	0.191	5.2	60.0	85.7	84.1	1.9	23.3	0.7	0.7	0.9	0.7
	0.4	53399.3	0.225	4.8	60.0	85.7	83.4	1.9	19.8	0.7	0.7	0.9	0.7
	0.5	19954.8	0.259	4.4	59.9	85.5	82.5	1.8	16.3	0.7	0.7	0.9	0.7
	0.6	8725.5	0.294	3.9	59.5	85.0	81.0	1.8	12.8	0.7	0.7	0.9	0.7
	0.7	4137.5	0.328	3.3	58.5	83.6	78.5	1.8	9.3	0.7	0.7	0.9	0.7
	0.8	1966.9	0.362	2.6	55.9	79.9	73.6	1.7	5.8	0.7	0.7	0.9	0.7

614

615

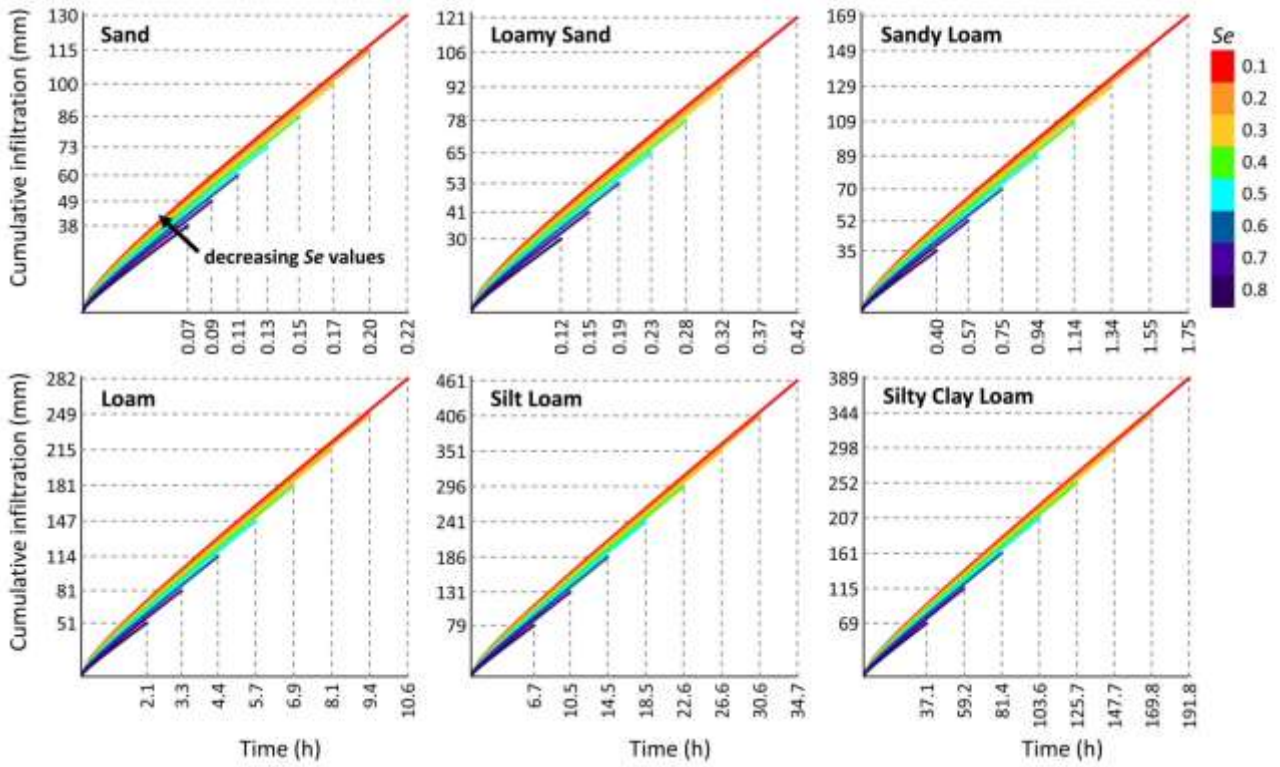
616 **Table Q.** Summary of the soil hydraulic properties estimated from the Beerkan database.

Statistic	λ_c (mm) (Eq. 8)	K_s (mm h ⁻¹)				
		BEST-steady (Eq. 15)	OPD (Eq. t1)	WU2 (Eq. t2)	SSBI (Eq. t3)	A4 (Eq. t4)
<i>N</i>	427	427	427	427	427	427
min	1.5	1.3	1.4	1.4	1.6	1.2
max	737.7	3550.9	3294.1	3493.8	3758.7	3173.7
mean	112.6	270.7	258.5	269.3	305.2	244.6
median	68.0	156.8	153.3	156.4	182.4	142.0
CV	101.3	142.0	140.1	141.3	137.6	141.3

617

618

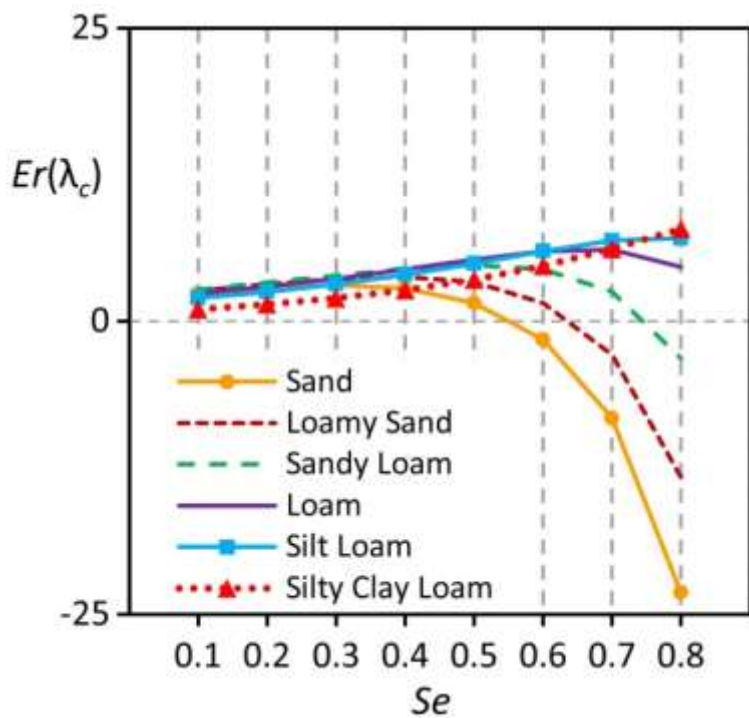
619 **Figure H.** Cumulative infiltration curves for different soils and initial effective saturation degrees, Se . The
 620 curve were generated analytically using Eqs. (10) and (11) and the parameters listed in **Table C**. The
 621 labels in ordinate and abscissa report respectively the total infiltrated water and the duration of the
 622 infiltration process. Note that the duration was fixed at three times the maximum time ($3 \times t_{max}$).



623

624

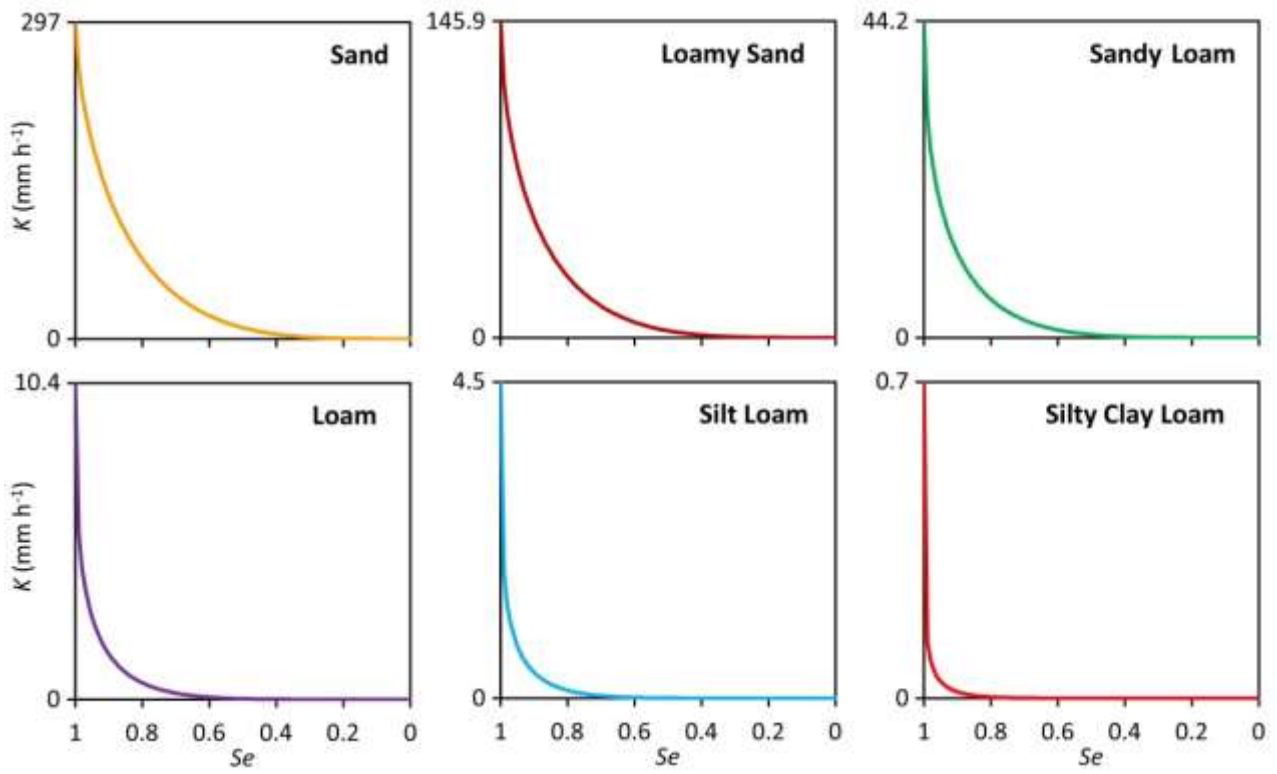
625 **Figure G.** Values of the relative error of the macroscopic capillary length, $Er(\lambda_c)$, predictions (expressed as a
626 percentage of the actual values, $\hat{\lambda}_c$) estimated for the six synthetic soils listed in **Table C**.



627

628

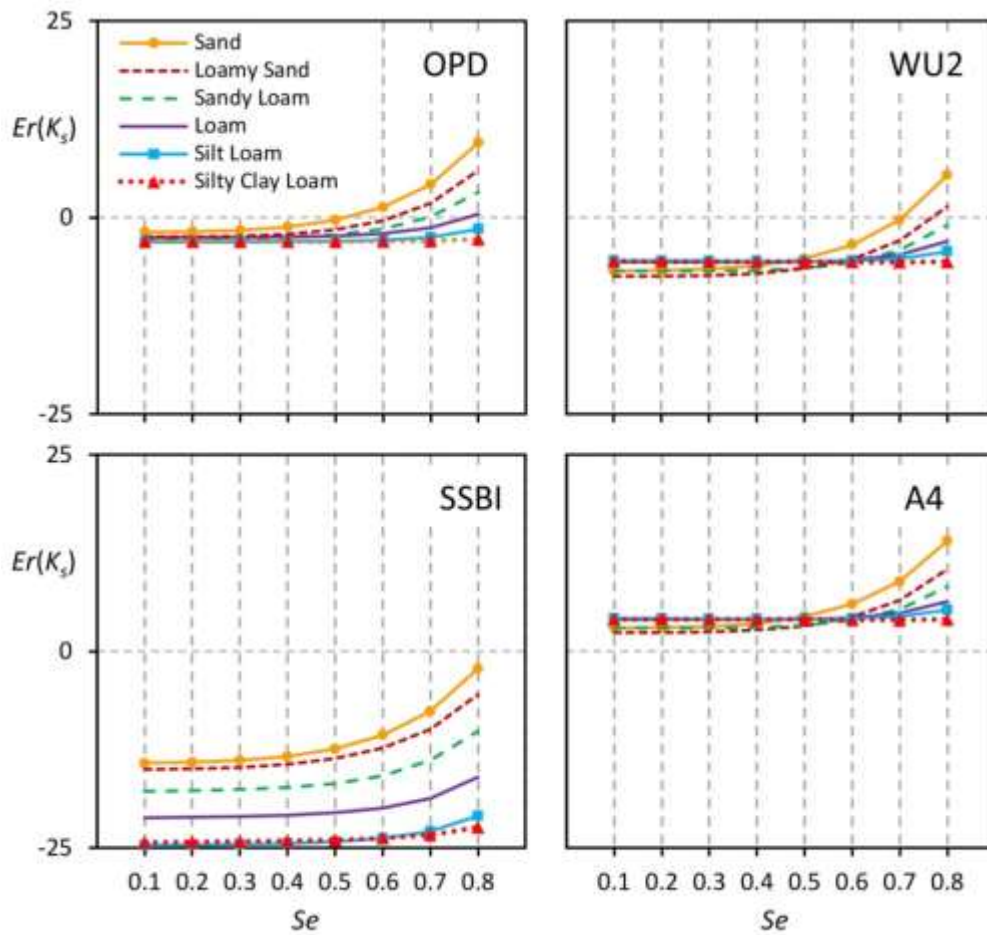
629 **Figure K.** Hydraulic conductivity functions of the six synthetic soils listed in **Table C.**



630

631

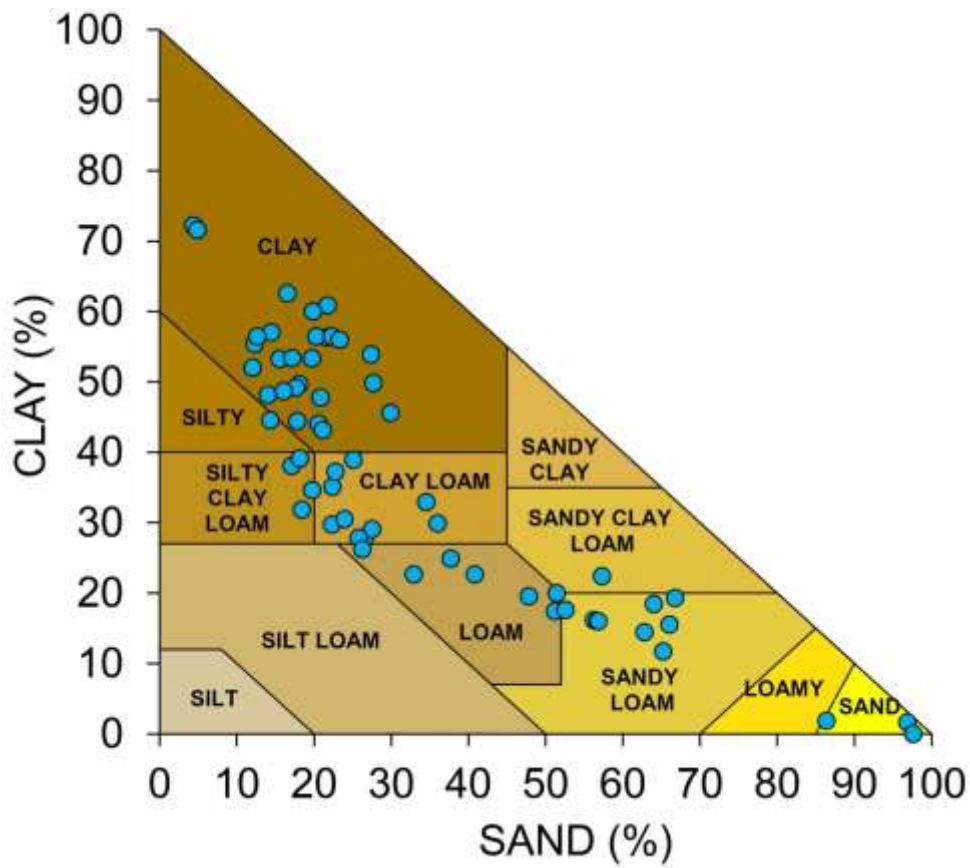
632 **Figure W.** Values of the relative error of the saturated soil hydraulic conductivity, $Er(K_s)$, predictions
 633 (expressed as a percentage of the actual values, \hat{K}_s) estimated for the six synthetic soils by the four
 634 considered methods (i.e., OPD, WU2, SSBI, A4).



635

636

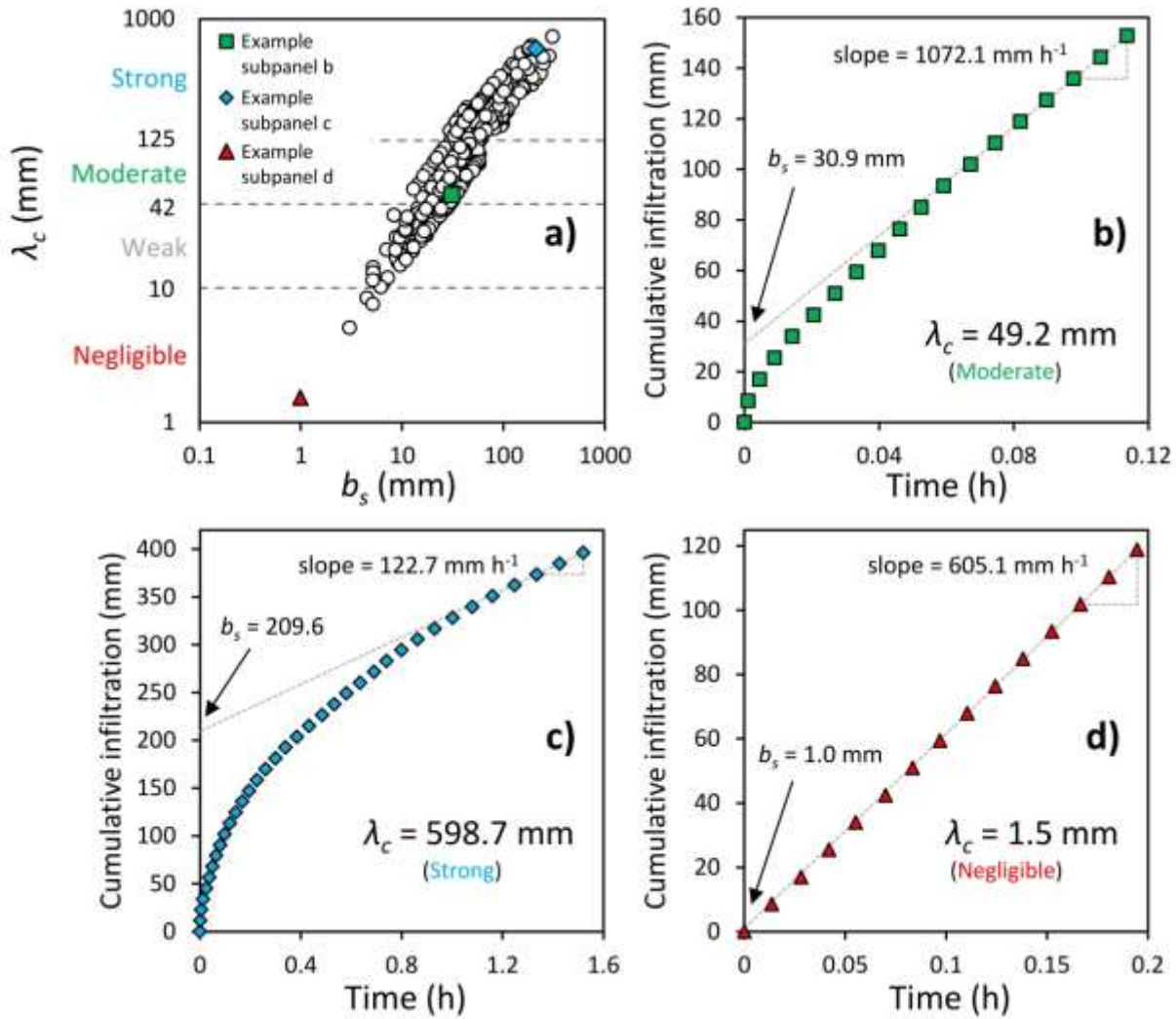
637 **Figure T.** Textural triangle and textural properties of the soils included in the Beerkan infiltration database.



638

639

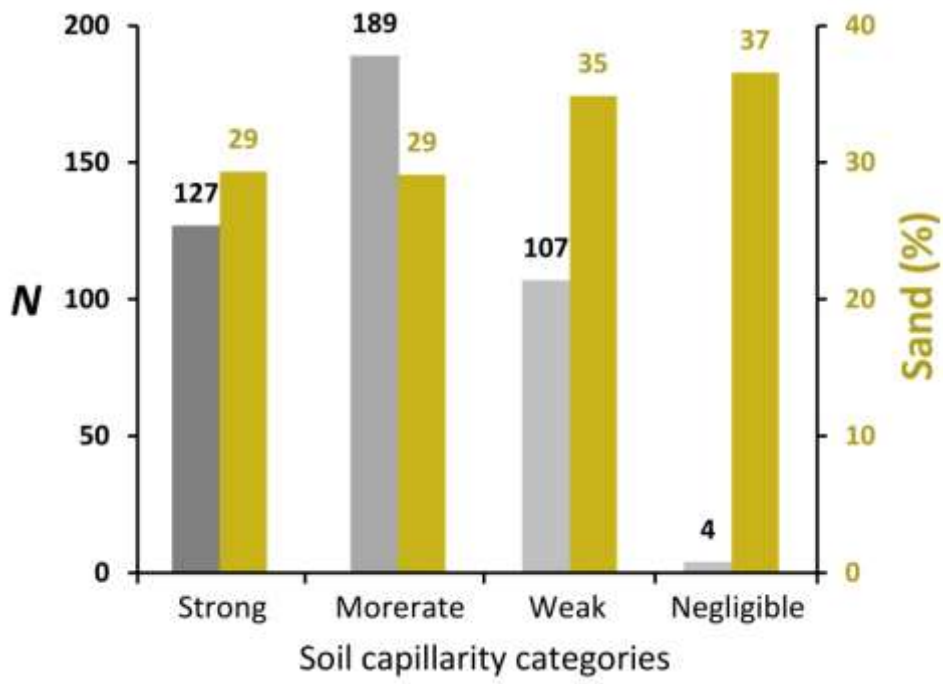
640 **Figure F. (a)** Comparison between the estimated macroscopic capillary length, λ_c , and the intercept, b_s ,
 641 values. The soil capillarity categories are also reported. **(a) (b) (c)** Examples of estimation of λ_c in case
 642 of **(b)** moderate, **(c)** strong, and **(d)** negligible capillarity conditions.



643

644

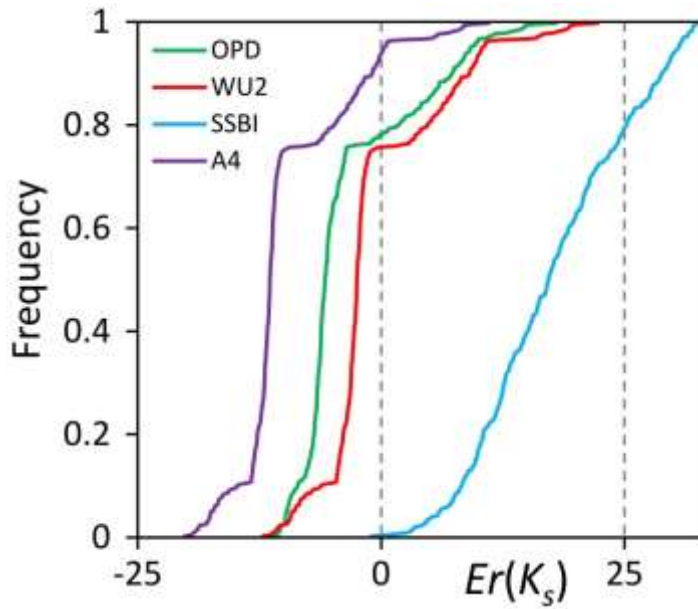
645 **Figure D.** Sample size, N , of the macroscopic capillary length predictions and mean sand content (%) for
646 each soil capillarity category.



647

648

649 **Figure Z.** Cumulative empirical frequency distribution of the saturated soil hydraulic conductivity, $Er(K_s)$,
650 predictions (expressed as a percentage of the BEST-deduced values, $K_{s,BEST}$), estimated for the six
651 considered soils by the four considered methods (i.e., OPD, WU2, SSBI, A4).



652